Induced Codeposition of Al–Mg Alloys in Lewis Acidic $AlCl_3$–EMIC Room Temperature Molten Salts

Masatsugu Morimitsu,* Nobutada Tanaka, and Morio Matsunaga
Department of Applied Chemistry, Kyushu Institute of Technology, 1-1 Sensui, Tobata-ku, Kitakyushu 804-8550

(Received June 15, 2000; CL-000586)

Voltammetric measurements and elemental analyses of electrodeposits have revealed the induced codeposition of Al–Mg alloys in acidic $AlCl_3$–EMIC melts containing $MgCl_2$.

Aluminum–magnesium alloys have attractive properties such as low density, high strength, good corrosion resistance, and work-hardenability, and these account for their use in a wide variety of chemical-processing and food-handling equipments as well as structural applications involving exposure to seawater. The use of a thin film of Al–Mg alloy is cost-efficient, as well, and the thin film can be applied by cladding and hot dip coating techniques. However, the thin film of alloy formed by these methods often shows the reduction in mechanical strength and corrosion resistance compared to the alloy as a bulk material. Electroplating is another option for the thin film coating of various kinds of alloys; it has been demonstrated that aluminum alloys such as Al–Mn,[1,2] Al–Ni,[3,4] Al–Ti,[5] Al–Co,[6,7] and Al–Cr[8–10] can be electroplated from chloroaluminate molten salts. Recently, room temperature molten salts, which are obtained by mixing of anhydrous aluminum chloride with either 1-ethyl-3-methylimidazolium chloride (EMIC) or *n*-butylpyridinium chloride (BPC), have attracted considerable attention as solvents for aluminum alloy deposition.[4,6–9] The electrodeposition of the above mentioned aluminum alloys in the chloroaluminate melts is reasonable from thermodynamic perspectives, since a metal nobler than aluminum is codeposited with aluminum for each of those alloys. On the other hand, the standard potential of the Mg(II)/Mg couple is much lower than that of the Al(III)/Al couple. Therefore, the electrodeposition of Al–Mg alloys in the melts seems implausible and in fact, with the exception of a technical document,[11] there have been no relevant papers published on the topic. This situation motivated us to attempt to confirm the possibility of the deposition of Al–Mg alloys in room temperature chloroaluminate melts. We carried out voltammetric studies on the cathodic reactions in Lewis acidic $AlCl_3$–EMIC melts containing $MgCl_2$. The structure and composition of the deposits obtained from the melt were then analyzed.

The procedures for preparing and purifying $AlCl_3$–EMIC melts are described in a previous paper.[8] Anhydrous $MgCl_2$ (Aldrich, 99.99%) was used as received. $MgCl_2$-added melts were prepared by dissolving 0.2 mol kg^{-1} $MgCl_2$ in a 2:1 (mole ratio) $AlCl_3$–EMIC melt. Voltammetric measurements in the $MgCl_2$-added melt were performed using a three-electrode glass cell. The working electrode was a Pyrex glass-shrouded tungsten wire (1 mm diam) and the counter electrode was a coiled tungsten wire. An aluminum wire immersed in a 2:1 $AlCl_3$–EMIC melt was used as the reference electrode and was separated from the bulk solution by a fine glass frit (Ace Glass, porosity E). Inductively coupled plasma spectrometry (ICPS) was used to assess the elemental composition of electrodeposits. Samples for ICPS analysis were prepared by constant current electrolyses using a Pyrex glass cell equipped with two platinum flag electrodes. After the electrodeposits were removed from the melt, they were soaked in benzene to remove residual melt. They were then dissolved in dilute aqueous nitric acid and analyzed for their aluminum and magnesium contents. Structural analyses of the electrodeposits were undertaken with X-ray diffraction using Cu-Kα radiation. The cells used in this study were sealed under vacuum after the melts had been loaded in an argon-filled globe box. All electrochemical experiments were conducted with an EG&G Model 273 potentiostat/galvanostat controlled by a personal computer equipped with EG&G Model 270 software. Electronic compensation of electrolyte resistance was employed during voltammetric experiments. The temperature was controlled at 30 ± 1 °C with Omron temperature controller Model E5AJ-A2AB.

Figure 1 shows the cyclic voltammograms of 2:1 $AlCl_3$–EMIC melts with and without $MgCl_2$. The cyclic voltammogram of the pure $AlCl_3$–EMIC melt showed a reduction wave on the forward scan and a single symmetrical oxidation wave on the reverse scan, which respectively correspond to the deposition and stripping of pure aluminum. The onset potential of the pure aluminum deposition was ca. 0.23 V less than the reversible potential of the Al(III)/Al couple. This large overpotential is attributed to the three-dimensional nucleation process for the electrodeposition of aluminum,[12] which is suggested in Figure 1 by a crossover loop following scan reversal in the –0.25 to –0.12 V potential region. When $MgCl_2$ was added to the melt, the deposition process was promoted such that the same deposition current was obtained at more positive

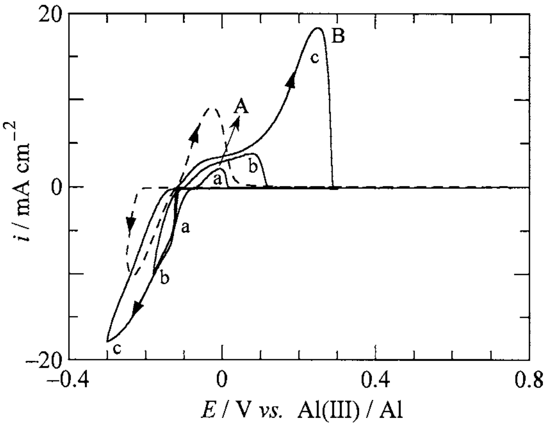

Figure 1. Cyclic voltammograms of 2:1 $AlCl_3$-EMIC melts with (solid curves) and without (dashed curve) 0.2 mol kg^{-1} $MgCl_2$ at 30 ℃. Scan rate, 2 mV s^{-1}. Switching potential, -0.13 V (a), -0.18 V (b), -0.30 V (c).

potentials. Moreover, the voltammetric features after scan reversal in this melt were highly dependent on the switching potential; i.e., the potential at which the voltammetric scan was reversed. The voltammogram with the switching potential of –0.13 V exhibited a reduction current starting at ca. –0.12 V with a crossover loop after the scan reversal. A single oxidation wave (wave A) appeared in the same potential region as the oxidation wave for the pure aluminum dissolution. When the potential scan was reversed at –0.18 V, the voltammogram presented a cathodic wave without a crossover loop and an asymmetric anodic wave that presumably consisted of the superimposition of two anodic waves. These anodic waves were successfully divided in the voltammogram when the switching potential was –0.30 V: along with the preceding anodic wave (wave A), a well-defined anodic wave (wave B) with a peak potential of ca. 0.25 V, more positive than that of the pure aluminum dissolution, was seen.

Because of the similarity of the first oxidation wave (wave A) obtained in the $MgCl_2$-added melt to the anodic wave of the pure melt, this oxidation wave can presumably be attributed to aluminum dissolution Therefore, the cathodic reaction in the $MgCl_2$-added melt starts with aluminum deposition, of which the overpotential is reduced by the addition of $MgCl_2$. The decrease in the overpotential of the aluminum deposition is unpredicted, since $MgCl_2$ partially buffers an acidic $AlCl_3$–EMIC melt[13]; i.e., $MgCl_2 + 2\ Al_2Cl_7^- \rightarrow Mg^{2+} + 4\ AlCl_4^-$. This reaction induces a decrease in $Al_2Cl_7^-$ concentration, resulting in a negative shift of the aluminum deposition potential. Therefore, the presence of Mg^{2+} can be considered to reduce the overpotential of the aluminum deposition attributed to the nucleation process, although the mechanism by which this happens is unknown at present. Another cathodic reaction following the aluminum deposition is suggested by the appearance of wave B, for which the reaction process obviously differs from the dissolution of pure aluminum. This was successfully confirmed by ICPS analyses of the deposits obtained by constant current electrolyses. Figure 2 displays the Mg atomic ratios of the deposits obtained at different cathodic current densities. The result clearly indicates that Al–Mg alloys can be electrodeposited in the $MgCl_2$-added melt and that the Mg atomic ratio increases with increasing current density; i.e., with increasing cathodic overpotential. Therefore, wave B corresponds to the dissolution process of Al–Mg alloys. The alloy deposits obtained in this study were single-phase Mg-containing Al solid solutions: their XRD patterns were almost identical to that of pure aluminum, irrespective of their Mg atomic ratio. This is reasonably understood by the fact that the Mg atomic ratio in the present study is relatively low, less than 2.2 at.%.

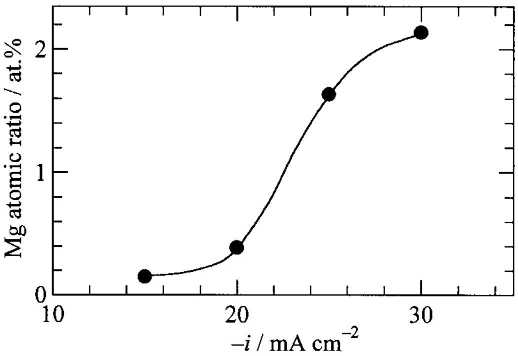

Figure 2. Atomic ratios of Mg in the electrodeposits obtained on a platinum electrode at different current densities in a 2:1 $AlCl_3$-EMIC melt containing 0.2 mol kg^{-1} $MgCl_2$ at 30 ℃. The charge passed was 7.2 C cm^{-2}.

The electrodeposition of Al–Mg alloys in an acidic $AlCl_3$–EMIC melt is quite intriguing, because thermodynamics seems not to allow magnesium to codeposit with aluminum due to the order of their standard potentials. However, Al–Mg alloy deposition is not limited to the present case: e.g., this alloy can be electrodeposited from organometallic electrolytes containing KF, $(C_2H_5)_2Mg$, $(C_2H_5)_3Al$, *iso*-$(C_4H_9)_3Al$, and toluene.[14] In addition, it is known that some kinds of alloys, such as tungsten or molybdenum alloys with transition metal, can be deposited from aqueous solutions, although their electrodepositions are not expected thermodynamically. Brenner has classified this type of alloy deposition as an "induced codeposition," of which one of the typical features is a positive shift in deposition potential; i.e., the alloy deposition occurs at more positive potentials than the deposition of the more noble metal (i.e., the inducing metal) of the alloy components.[15] As mentioned above, such a potential shift was observed for Al–Mg alloy deposition. Therefore, it is concluded that the induced codeposition of magnesium with aluminum can occur in acidic $AlCl_3$–EMIC melts containing $MgCl_2$. Further the present results suggest the potential of the electrodeposition of Al–Mg based ternary alloys, such as Al–Mg–Mn, Al–Mg–Cr, and Al–Mg–Zn, in acidic $AlCl_3$–EMIC melts.

References

1 G. R. Stafford, *J. Electrochem. Soc.*, **136**, 635 (1989).
2 B. Grushko and G. R. Stafford, *Met. Trans.*, **21A**, 2869 (1990).
3 T. P. Moffat, *J. Electrochem. Soc.*, **136**, 3059 (1994).
4 W. R. Pitner, C. L. Hussey, and G. R. Stafford, *J. Electrochem. Soc.*, **136**, 130 (1996).
5 G. M. Janowski and G. R. Stafford, *Met. Trans.*, **23A**, 2715 (1992).
6 R. T. Carlin, P. C. Trulove, and H. C. De Long, *J. Electrochem. Soc.*, **143**, 2747 (1996).
7 M. R. Ali, A. Nishikata, and T. Tsuru, *Electrochim. Acta*, **42**, 1819 (1997).
8 M. Matsunaga, M. Morimitsu, N. Nagano, and T. Tsuda, *Molten Salt Forum*, **5–6**, 601 (1998).
9 M. R. Ali, A. Nishikata, and T. Tsuru, *Electrochim. Acta*, **42**, 2347 (1997).
10 T. P. Moffat, *J. Electrochem. Soc.*, **141**, L115 (1994).
11 S. Takahashi, M. Nishihata, and K. Oku, Jpn. Patent 3033596 (2000).
12 R. T. Carlin, W. Crawford, and M. Bersch, *J. Electrochem. Soc.*, **139**, 2720 (1992).
13 P. Koronaios and R. A. Osteryoung, *J. Electrochem. Soc.*, **146**, 2995 (1999).
14 A. Mayer, *J. Electrochem. Soc.*, **137**, 2806 (1990).
15 A. Brenner, "Electrodeposition of Alloys," Academic Press, New York (1963), Vol. 1, Chap. 6, p. 78; Chap. 12, p. 348.